



Cite this: *RSC Adv.*, 2017, 7, 47636

Surface treatment of halloysite nanotubes with sol–gel reaction for the preparation of epoxy composites

Taehee Kim, Suhyun Kim, Dong Koo Lee, Bongkuk Seo* and Choong-Sun Lim *

Halloysite nanotubes (HNTs) are naturally occurring aluminosilicates that have received attention for their high aspect ratio and low cost, which makes them suitable for commercial applications. HNTs provide good mechanical properties when applied in epoxy resins as fillers. The mechanical and thermal properties of HNTs are further enhanced by surface treatment using the sol–gel method. In this study, the modified surfaces of HNTs (m-HNTs) were investigated using scanning electron microscopy and transmission electron microscopy. The amounts of m-HNTs were varied in the epoxy composition (binder) that was comprised of a latent hardener, a reaction accelerator, and an epoxy resin. The physical properties of the cured composites with different amounts of HNTs and m-HNTs were measured using a universal testing machine (UTM) to analyze the effect of HNT and m-HNT on the flexural strength. Furthermore, the thermomechanical analysis of the cured composites with m-HNT showed that the dimensional changes of the composites were lower than those of epoxy composites with HNT particles.

Received 17th August 2017
 Accepted 2nd October 2017

DOI: 10.1039/c7ra09084f

rsc.li/rsc-advances

1. Introduction

Epoxy resins have a wide range of applications in the aerospace, automotive, and construction industries owing to their good mechanical and thermal properties as well as their convenience of use.^{1–3} Epoxy resins form networked thermoset polymers with properties that are useful in epoxy molding compounds or adhesives.^{4,5} However, epoxy polymers suffer from brittleness, low thermal conductivity, and high flammability.^{6–8} Such drawbacks can be compensated for by incorporating tougheners, additives, or fillers into the polymer. The low viscosity of epoxy resins allows incorporation of high filler contents into the cured matrix, which can result in improved flame resistance and mechanical properties of the epoxy composite.^{9,10}

Halloysite nanotubes (HNTs) are naturally occurring clay minerals sharing the same chemistry as that of kaolinite, $\text{Al}_2(\text{OH})_4\text{Si}_2\text{O}_5 \cdot n\text{H}_2\text{O}$.¹¹ In general, HNTs consist of two nanosheets forming a multilayered tubular structure. The outer layer of HNT is composed of tetrahedral siloxane (Si–O–Si) with a few Al–O and Si–OH groups, whereas the internal layer is composed of octahedral aluminol (Al–O–Al).^{12,13}

Polymer composites for industrial applications require mechanical or thermal properties such as high flexural strength and dimensional stability to resist deformation caused by applied stress arising from changes in temperature. Fillers such as modified graphene or carbon nanotubes (CNTs) have been

often added to improve the mechanical or thermal properties of polymers.^{14,15} However, the process complexity and high production costs have been major hurdles. Unlike the expensive nanofillers, HNT is a naturally abundant, highly available, low-cost, and promising material with a high aspect ratio that can improve the mechanical properties, thermal stability, and flame retardancy of polymer composites.^{16,17}

Numerous surface modification studies on HNTs have been carried out because the targeted properties could be enhanced for specific applications by selectively modifying the external, internal, and interlayer surfaces of HNT. Surface modifications of the external HNT layers were previously achieved by adsorption of cationic polyethyleneimine based polymers onto the negatively charged external surface of HNTs.^{18,19} In addition, a silanol amine²⁰ or ionic liquids were used for the surface modification of HNTs.²¹ On the internal surfaces of HNT, Al–OH groups with high chemical activity react with 3-aminopropyltriethoxysilane to form a 3-aminopropyl layer during a sol–gel process.¹³ The interlayer surfaces of HNTs or kaolinite bind with water or other layers *via* hydrogen bonds. Therefore, prior treatments are required before surface modifications to weaken the interlayer hydrogen bonding. The intercalation of organic compounds such as DMSO followed by methanol intercalation introduces methoxy groups into the interlayer space that can serve as a host for guest molecules.²²

Although various surface treatment approaches for polymer modification on HNTs have been studied, there are few surface modifications reported with metal oxides. Here, we report the growth of silica nanoparticles on the HNT surface using sol–gel reaction. The modified surface of HNTs was analyzed using field

Center for Chemical Industry Development, Korea Research Institute of Chemical Technology, Ulsan 44412, Korea (ROK). E-mail: bksea@kricr.re.kr; chsunlim@kricr.re.kr



emission scanning electron microscopy (FE-SEM) and field emission transmission electron microscopy (FE-TEM). To measure the property changes in the polymer composites that contain HNTs and m-HNTs, an epoxy binder was prepared by blending diglycidyl ether of bisphenol A (DGEBA), dicyandiamide (dicy), and a catalyst, 1,1-dimethyl-3-phenyl urea (DPU). Different amounts of modified HNTs were added to the epoxy binder and cured into epoxy composites to measure their flexural strength using a universal testing machine (UTM) as well as dimensional stability by measuring the linear coefficient of thermal expansion (CTE) using thermomechanical analysis (TMA).

2. Material and methods

2.1 Materials

Tetraethyl orthosilicate (TEOS), dicy, and DPU were purchased from Sigma-Aldrich (USA). Diglycidyl ether of bisphenol A (epoxy equivalent weight of 187) was bought from Momentive Co. HNTs were obtained from Applied Minerals. The length, outer diameter, and inner diameter of the HNTs were 0.2–2 μm , 50–70 nm, and 15–45 nm, respectively.

2.2 Surface modification of HNT

HNTs (3 g) were added to a 200 mL mixture of ethanol (EtOH) and H_2O at a vol/vol ratio of 50 : 50 and stirred for 3 h under sonication. TEOS (10 mL), and NH_3OH (16 mL) were added into the solution and stirred for 5 h. Modified HNTs (m-HNTs) were finally dispersed in a mixture of EtOH/ H_2O . A drop of the suspended m-HNTs was placed on a silicon wafer and a TEM grid for SEM and TEM characterization, respectively.

2.3 Formulation and curing methods of epoxy compositions with HNTs

DGEBA (100 phr, part per resin) and the curing agent dicy (11.2 phr) were mixed in a stoichiometric ratio while HNT or m-HNT was added from 0 to 25 wt% with an increment of 5 wt%. DPU was added at 0.21 phr into each composition. Detailed information is presented in Table 1. The mixtures were dispersed with three roll mills followed by stirring with a mechanical overhead stirrer for 30 min at 70 $^\circ\text{C}$ under vacuum. The prepared epoxy pastes were poured into metal molds and heated for 30 min at 170 $^\circ\text{C}$ and for 2 h at 190 $^\circ\text{C}$ for complete curing.

2.4 Characterization

The morphologies of both HNTs and m-HNTs were studied with FE-SEM (Mira3, Tescan) and FE-TEM (JEM-2010, JEOL, and Talos F200S) equipped with energy dispersive X-ray spectroscopy (EDX). The cured epoxy composites were processed into 60 mm \times 25 mm \times 3 mm specimens and tested ten times using the method ASTM D 790M repeatedly to measure flexural strength with a UTM (UTM 5982, Instron). The linear CTE was analyzed using the TMA (Q400, TA Instruments) with a 5 mm \times 5 mm \times 3 mm test specimen. The test temperature was increased at a rate of 2 $^\circ\text{C min}^{-1}$ from 25 to 200 $^\circ\text{C}$. The change in T_g was measured with differential scanning calorimetry (DSC) (Q-200, TA Instruments) by heating the samples at a heating rate of 10 $^\circ\text{C min}^{-1}$ from 25 to 300 $^\circ\text{C}$ followed by cooling to -80 $^\circ\text{C}$ at a rate of -10 $^\circ\text{C min}^{-1}$. The same samples were heated again to 300 $^\circ\text{C}$ at a rate of 10 $^\circ\text{C min}^{-1}$ to obtain T_g data.

3. Results and discussion

The SiO_2 particles on HNTs were grown by sol-gel reactions between Si-OH groups on the HNT surface and TEOS. A sol-gel reaction scheme between HNTs and TEOS is displayed in Fig. 1. The silanol OH reacts with ethoxyl groups on TEOS, forming siloxane groups that grow into discrete silica particle structures. The small silica particles attached to the HNT surface can improve the rigidity and thermal stability of HNTs. The synthesized silica particles were characterized by FE-SEM and TEM, as shown in Fig. 2. The characterization results acquired from SEM, TEM, and EDX for unreacted HNTs and m-HNTs are shown in Fig. 2a–c and 2d–f, respectively. Fig. 2d and e show a significant growth of particles on the surface of HNTs as a result of sol-gel reactions, whereas no particles were observed on pristine HNTs, as shown in Fig. 2a and b. According to the EDX spectra, m-HNTs show a significantly increased Si/Al ratio compared to HNTs, which confirms the SiO_2 particle modification on the m-HNT surfaces (Fig. 2c and f).

Variable amounts of m-HNTs and pristine HNTs were added to epoxy compositions containing epoxy resin, dicy, and DPU to prepare epoxy composites, as given in Table 1. The T_{peak} value for the compositions measured by DSC was in the temperature range of 171–188 $^\circ\text{C}$, which is similar to the curing temperature shown in Fig. 3. The information is provided in Table 2. In Table 2, the T_g of H-5 decreased by 6 $^\circ\text{C}$, but as the amount of HNT increased, the T_g of H-10, and

Table 1 The compositions of epoxy composites

| | Reference | HNT-5% | | HNT-10% | | HNT-15% | | HNT-20% | | HNT-25% | |
|----------------------|-----------|--------|-------|---------|-------|---------|-------|---------|--------|---------|-------|
| Sample name | Binder | H-5 | HS-5 | H-10 | HS-10 | H-15 | HS-15 | H-20 | HS-20 | H-25 | HS-25 |
| Epoxy resin | 100 | 100 | 100 | 100 | 100 | 100 | 100 | 100 | 100 | 100 | 100 |
| dicy | 11.24 | 11.24 | 11.24 | 11.24 | 11.24 | 11.24 | 11.24 | 11.24 | 11.24 | 11.24 | 11.24 |
| DPU | 0.21 | 0.21 | 0.21 | 0.21 | 0.21 | 0.21 | 0.21 | 0.21 | 0.21 | 0.21 | 0.21 |
| HNT | — | 5.86 | — | 12.38 | — | 19.68 | — | 27.875 | — | 37.15 | — |
| HNT-SiO ₂ | — | — | 5.86 | — | 12.38 | — | 19.68 | — | 27.875 | — | 37.15 |



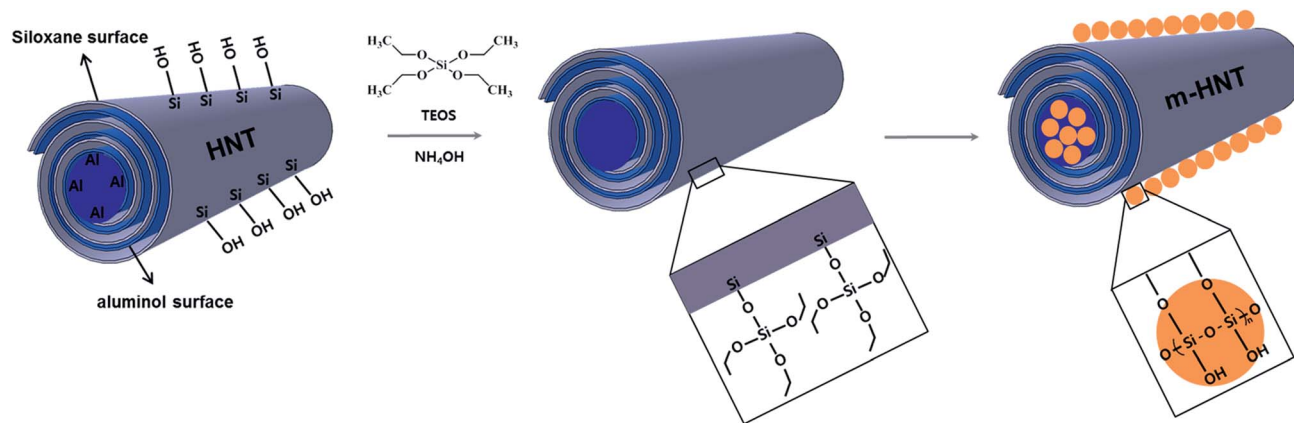


Fig. 1 HNT structure and reaction scheme of sol-gel process, in which TEOS reacts with silanol OH groups on HNT, forming SiO_2 modified m-HNT.

H-15 gradually increased and became similar to that of binder at H-15. It indicates that though increasing amount of HNT forms better interaction with polymer matrix, pure HNTs are not well dispersed in the polymer matrix. For HS-5, its T_g also decreases but T_g of HS-10 becomes maximized to 134°C . It suggests that m-HNTs are well dispersed in the epoxy polymer.

The cured epoxy composites were processed to make test specimens for flexural strength tests to measure the maximum

stress each composite can withstand. The flexural strength measurement results show that the flexural strength of the epoxy composites increases with an initial increase in HNT and m-HNT contents for composites with pristine HNTs and m-HNTs, respectively (Fig. 4). The flexural strength of epoxy composites with m-HNT remained slightly higher than that of pristine HNT up to 15 wt%. However, an increase from 15 wt% to 20 wt% in HNT content resulted in a sharp decrease of the strength of HNT composites (H-composites) while the strength

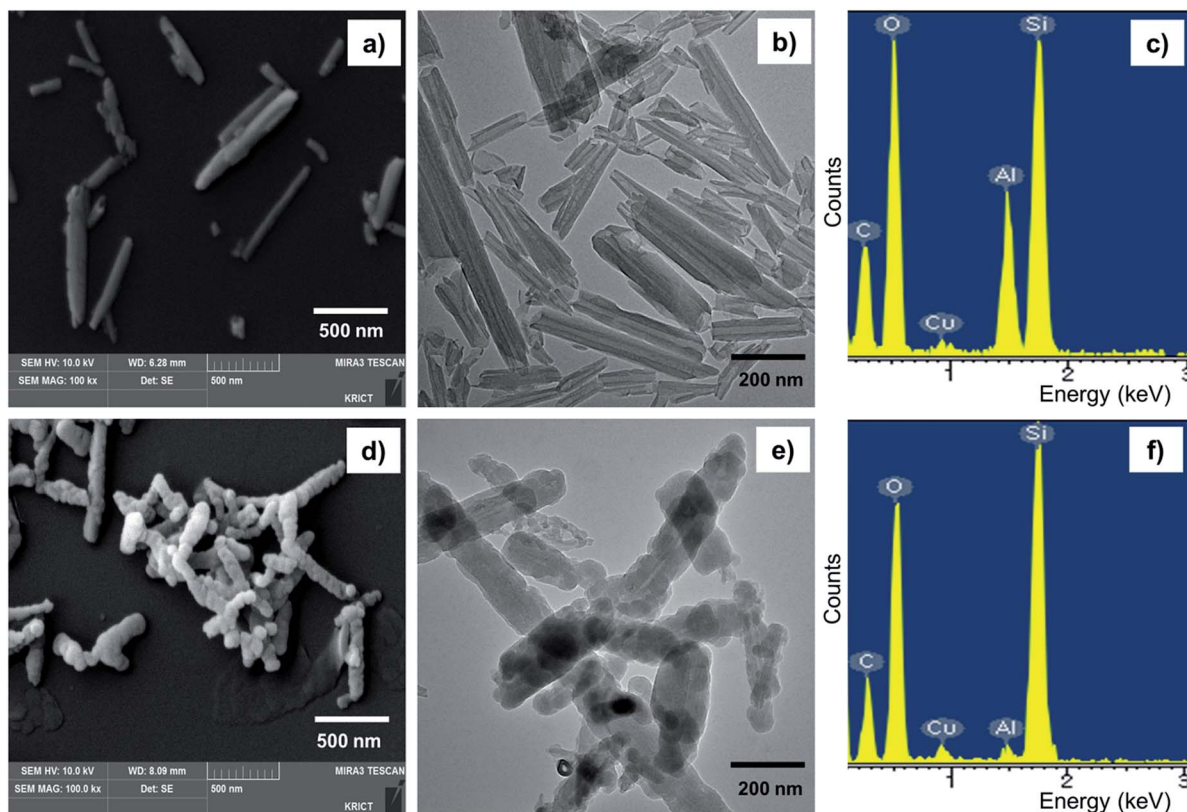


Fig. 2 (a) FE-SEM and (b) TEM images of HNT and (c) EDX spectrum acquired for HNT. (d) FE-SEM and (e) TEM images of m-HNT and (f) EDX spectrum acquired for m-HNT.



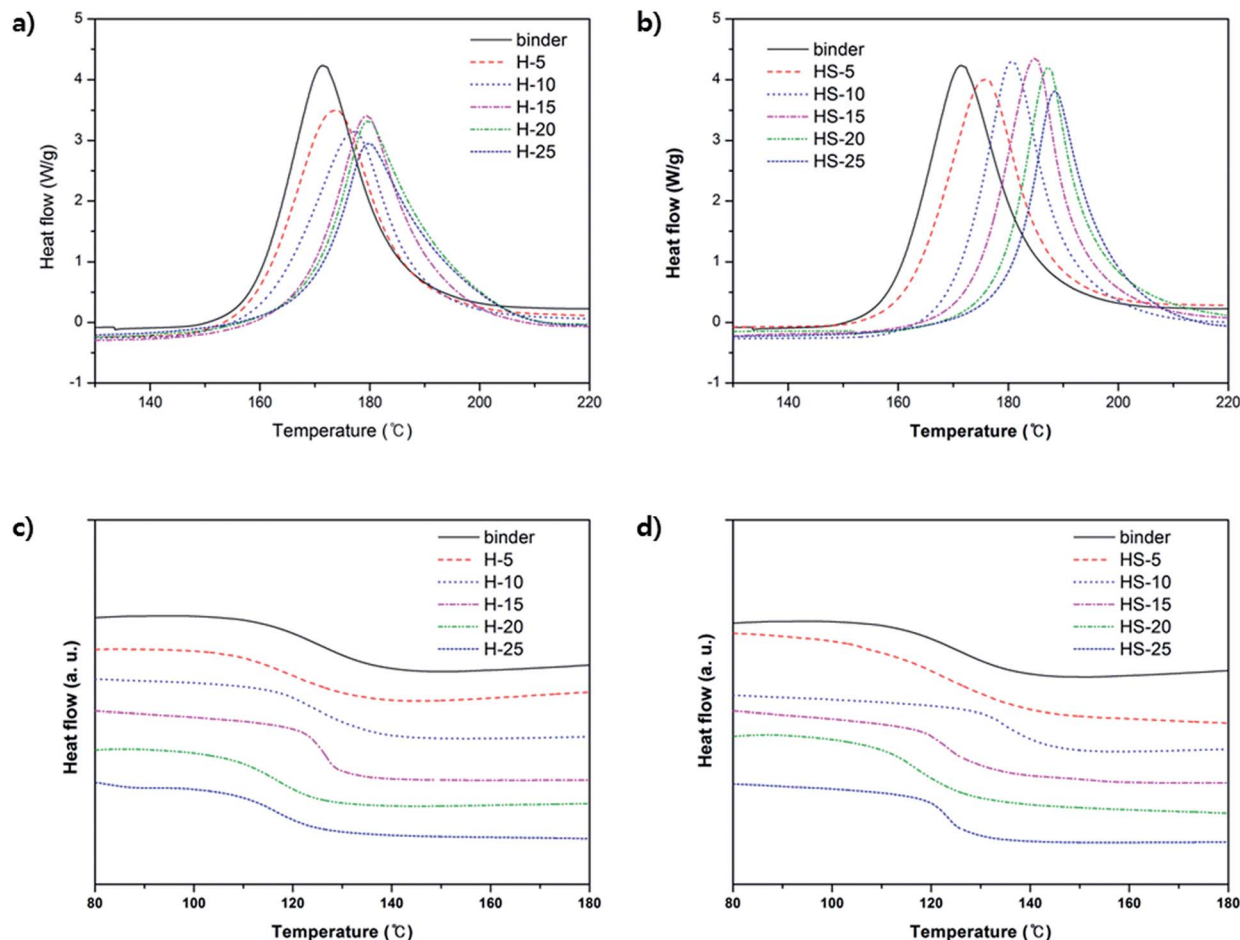


Fig. 3 DSC graphs of epoxy composites with various compositions. First run of (a) H-composites and (b) HS-composites. Second run of (c) H-composites and (d) HS-composites.

of m-HNTs composites (HS-composites) continued to increase. An increase from 20 wt% to 25 wt% in HNT content led to a decrease in the flexural strength of HS-composites, similar to that of H-composites at 15 wt%. This decrease is due to the excessive amount of filler in the composites, which tends to reduce their mechanical properties. The flexural strength measurement results indicate that the incorporation of m-HNT noticeably improves the mechanical

properties of epoxy composites compared to those with pristine HNT.

Thermomechanical properties of the epoxy composites were also analyzed by using TMA. TMA measures the linear

Table 2 DSC data of the epoxy composites with HNTs and m-HNTs

| Sample name | T_{peak} (°C) | T_{onset} (°C) | T_g (°C) |
|-------------|------------------------|-------------------------|------------|
| Binder | 171.44 | 154.08 | 126.68 |
| H-5 | 173.62 | 154.37 | 120.86 |
| H-10 | 176.85 | 155.82 | 123.04 |
| H-15 | 179.36 | 159.01 | 126.76 |
| H-20 | 179.72 | 163.27 | 115.56 |
| H-25 | 179.76 | 162.97 | 115.91 |
| HS-5 | 175.79 | 158.11 | 121.96 |
| HS-10 | 180.69 | 157.92 | 134.60 |
| HS-15 | 184.80 | 168.44 | 123.06 |
| HS-20 | 187.24 | 171.79 | 116.11 |
| HS-25 | 188.42 | 174.47 | 123.74 |

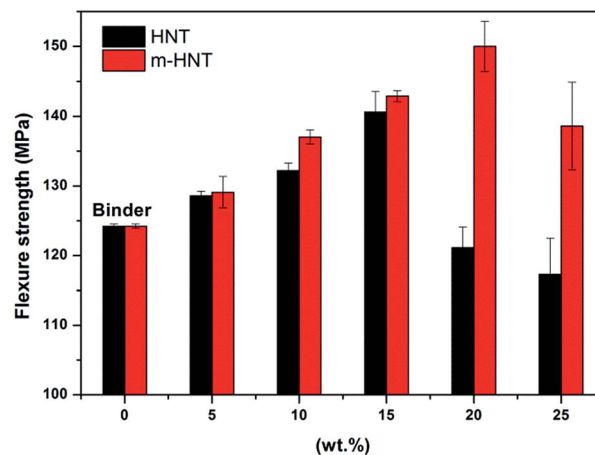


Fig. 4 Flexural strength of epoxy composites containing different amounts of HNT and m-HNT particles.



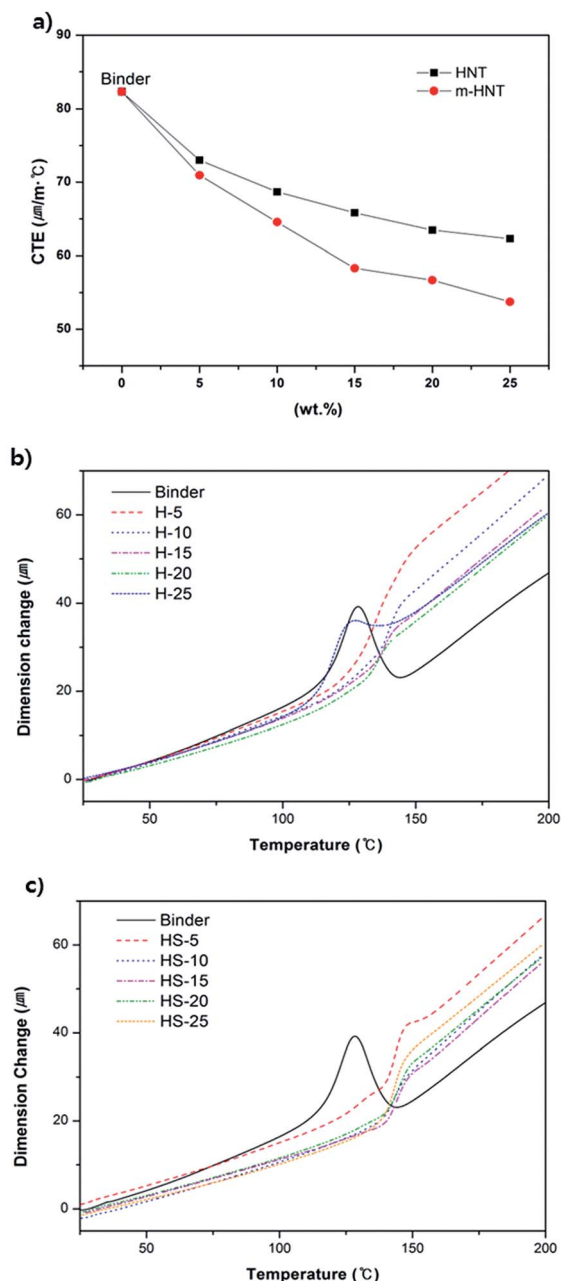


Fig. 5 (a) CTE vs. wt% and (b and c) dimensional change vs. temperature according to TMA.

dimensional change with respect to a change in temperature, inducing thermal expansion. The measured CTEs of the composites tend to decrease with an increase in HNT content from 5 wt% to 25 wt% (Fig. 5a). Furthermore, HS-composites show much lower CTE values than those of the H-composites as the contents of m-HNT and HNT increase (Table 3). The CTEs for HS- and H-composites at 20 wt% were 56.7 ppm K^{-1} and 63.4 ppm K^{-1} , respectively. The CTE decrease confirms that the dimensional stability of HS-composites was improved by the addition of m-HNT. The reduced CTE values of the HS-composites are a result of the synergistic influence

Table 3 CTE and T_g values of the HNT and m-HNT composites

| Sample name | α_1 (60–90 $^{\circ}\text{C}$, ppm K^{-1}) | α_2 (160–190 $^{\circ}\text{C}$, ppm K^{-1}) | T_g ($^{\circ}\text{C}$) |
|-------------|--|--|------------------------------|
| Binder | 82.3 | 150.0 | 143.4 |
| H-5 | 73.0 | 173.2 | 138.2 |
| H-10 | 68.6 | 172.1 | 140.2 |
| H-15 | 65.8 | 163.3 | 137.8 |
| H-20 | 63.4 | 160.3 | 136.1 |
| H-25 | 62.3 | 138.1 | 131.2 |
| HS-5 | 70.95 | 177.4 | 143.0 |
| HS-10 | 64.56 | 176.8 | 143.2 |
| HS-15 | 58.29 | 175.5 | 144.4 |
| HS-20 | 56.69 | 163.6 | 144.1 |
| HS-25 | 53.73 | 162.1 | 143.2 |

of the silica and HNT combination that decreased the dimensional changes. T_g values obtained from TMA indicate the temperature range in which the chain mobility in the free volume of the test specimen begins to increase sharply. The T_g value of HS-composites remained similar to that of the binder at 143°C , while the T_g value of H-composites was lower by approximately 6°C . A filler that interacts strongly with a polymer will be highly crosslinked within the polymer matrix, resulting in an increased T_g . According to Table 3, T_g was maintained at 143°C regardless of the increase in m-HNT content in the epoxy composites. Therefore, silica particles on m-HNTs have strong interactions with the hydroxyl group formed by the reaction between the amine curing agent and epoxy group. However, the T_g of the H-composites decreased from 143°C to 131.2°C with an increase in HNT content, which was due to the insufficient density of silanol OH groups on the surfaces of HNTs available for interaction with hydroxyl groups to restrain the polymer matrix from becoming rubbery. The T_g data obtained by the second DSC measurement also support the observation that the T_g of H-composites decreased proportionally with the amount of HNT, whereas the T_g of HS-composites remained almost the same regardless of the amount of m-HNT (Table 2 and Fig. 3c and d).

The effect of surface treatment of HNTs in the epoxy compositions was confirmed with the fractured surface images of cured epoxy compositions during Izod impact test (Fig. 6). The surface image of a cured epoxy binder (Fig. 6a) shows gentle surface, and Fig. 6b shows fractured surface with a cluster of pristine HNTs. Fig. 6c shows that the silica treated m-HNTs have so strong interaction with epoxy binder that m-HNTs are well dispersed in the cured epoxy matrix. Furthermore, the surfaces were observed with TEM. Pristine HNTs in HS-20 look aggregated while silica modified HNTs are well dispersed in epoxy polymer (Fig. 6d and e). Moreover, the entrance of modified HNT nanotube was monitored with TEM-EDS. The EDS analysis carried out along the line drawn at the top of the HNT (Fig. 6f) shows that silica nanoparticles are well distributed at the top of silica modified HNT.



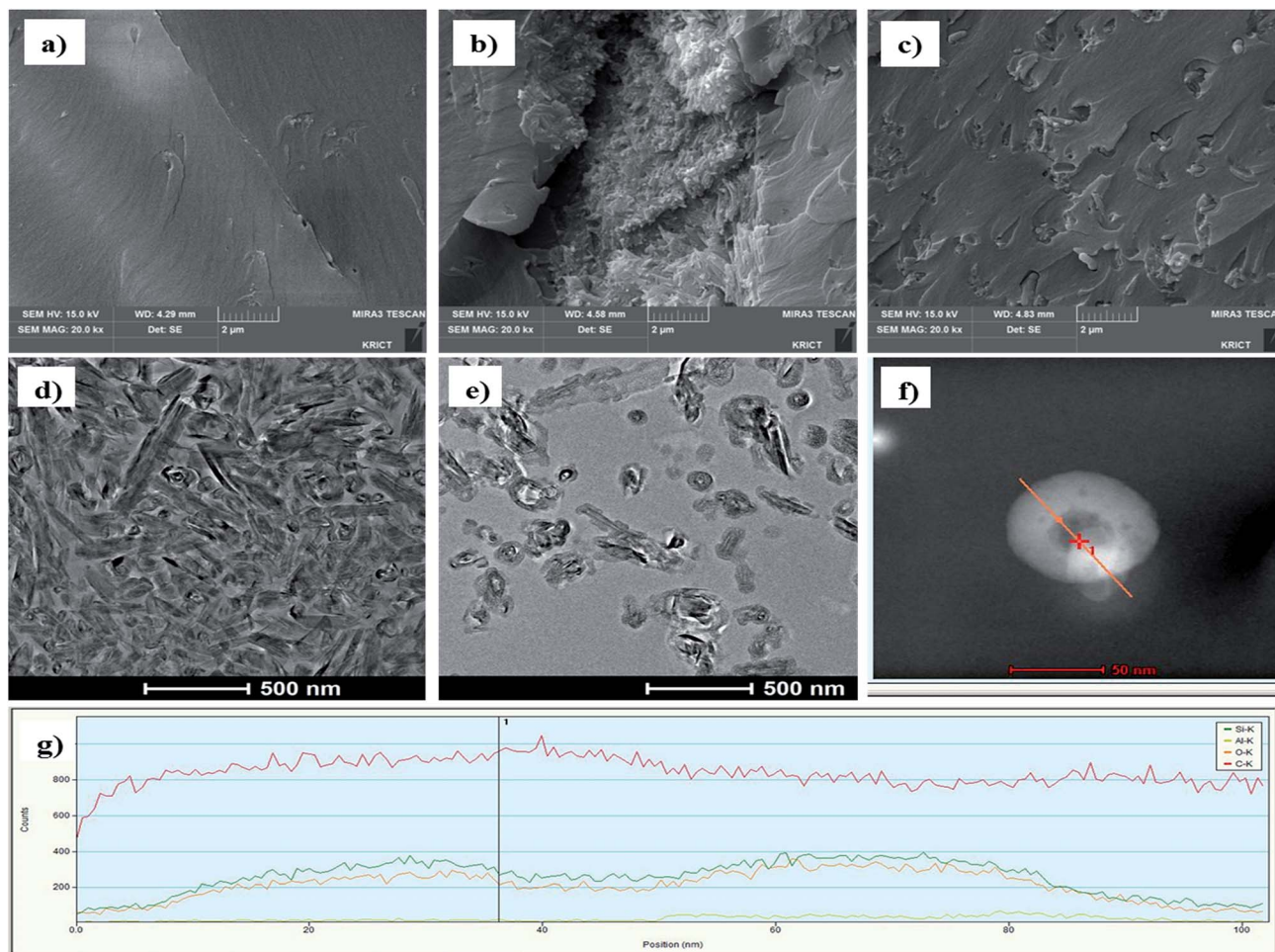


Fig. 6 FE-SEM images of the fractured surfaces of the cured epoxy compositions (a) binder, (b) H-5, and (c) HS-5. TEM images (d) H-20, (e) HS-20, (f) top view of silica nanoparticles modified HNT, and (g) EDS line scanning data of top view image.

Therefore, the entrance of nanotube is confirmed to be blocked with silica particles.

4. Conclusions

In this work, we studied the modification of HNTs by silica, using a sol-gel reaction and thermal and mechanical properties of the resultant epoxy composites containing silica-modified HNTs (m-HNTs) in comparison to those containing pristine HNTs. The SEM, TEM, and EDX characterization results for m-HNTs confirmed a successful modification of the HNT surface by silica particles. The flexural strength test results showed promising improvements for HS-composites as compared to the results for H-composites. In addition, encouraging improvements in the thermal properties of the composites were confirmed by the TMA results, according to which the dimensional stability of HS-composites was better than that of H-composites.

Conflicts of interest

There are no conflicts to declare.

Acknowledgements

This work was supported by the Korea Research Institute of Chemical Technology (KRICT) under the project "Development of specialty chemicals for automotive industry" (No. SI1709).

Notes and references

- 1 V. Baheti, J. Militky, R. Mishra and B. K. Behera, *Composites, Part B*, 2016, **85**, 268.
- 2 J. Feng and Z. Guo, *Composites, Part B*, 2016, **85**, 161.
- 3 E. Kuram, *Composites, Part B*, 2016, **88**, 85.
- 4 Z. Wang, P. Wei, Y. Qian and J. Liu, *Composites, Part B*, 2014, **60**, 341.
- 5 Y. Liu, H. V. Babu, J. Zhao, A. Goni-Urtiaga, R. Sainz, R. Ferritto, M. Pita and D. Y. Wang, *Composites, Part B*, 2016, **89**, 108.
- 6 K. Kim and J. Kim, *Int. J. Therm. Sci.*, 2016, **100**, 29.
- 7 S. M. Unlu, S. D. Dogan and M. Dogan, *Polym. Adv. Technol.*, 2014, **25**(8), 769.



- 8 E. D. Bain, D. B. Knorr, A. D. Richardson, K. A. Masser, J. Yu and J. L. Lenhart, *J. Mater. Sci.*, 2015, **51**(5), 2347.
- 9 R. T. Gomez-del, J. Rodríguez and R. A. Pearson, *Composites, Part B*, 2014, **57**, 173.
- 10 J. Gu, J. Dang, Y. Wu, C. Xie and Y. Han, *Polym.-Plast. Technol. Eng.*, 2012, **51**(12), 1198.
- 11 E. Joussein, S. Petit, J. Churchman, B. Theng, D. Righi and B. Delvaux, *Clay Miner.*, 2005, **40**(4), 383.
- 12 T. F. Bates, F. A. Hildebrand and A. Swineford, *Am. Mineral.*, 1950, **35**(7–8), 463.
- 13 P. Yuan, P. D. Southon, Z. Liu, M. E. R. Green, J. M. Hook, S. J. Antill and C. J. Kepert, *J. Phys. Chem. C*, 2008, **112**(40), 15742.
- 14 C. Zeng, S. Lu, L. Song, X. Xiao, J. Gao, L. Pan, Z. He and J. Yu, *J. Mater. Chem.*, 2015, **5**, 35773.
- 15 Y. Li, R. Umer, A. Isakovic, Y. A. Samad, L. Zheng and K. Liao, *J. Mater. Chem.*, 2013, **3**, 8849.
- 16 F. C. Chiu, *Composites, Part B*, 2017, **110**, 193.
- 17 M. Du, B. Guo and D. Jia, *Polym. Int.*, 2010, **59**(5), 574.
- 18 Y. Lvov, R. Price, B. Gaber and I. Ichinose, *Colloids Surf., A*, 2002, **198**, 375.
- 19 N. G. Veerabadran, D. Mongayt, V. Torchilin, R. R. Price and Y. M. Lvov, *Macromol. Rapid Commun.*, 2009, **30**(2), 99.
- 20 M. Sahnoune, A. Taguet, B. Otazaghine, M. Kaci and J. M. Lopez-Cuesta, *Eur. Polym. J.*, 2017, **90**, 418.
- 21 E. Bischoff, D. A. Simon, H. S. Schrekker, M. Lavorgna, L. Ambrosio, S. A. Liberman and R. S. Mauler, *Eur. Polym. J.*, 2016, **82**, 82.
- 22 Y. Komori, Y. Sugahara and K. Kuroda, *Chem. Mater.*, 1999, **11**(1), 3.

